JOURNAL OF MATERIALS SCIENCE 29 4750–4756

Measurement of the fracture toughness of polycrystalline diamond using the double-torsion test

TZE-PIN LIN, G. A. COOPER
Department of Materials Science and Mineral Engineering, University of California at Berkeley, CA 94720, USA

M. HOOD
Centre for Mining Technology and Equipment, Queensland Centre for Advanced Technologies, Queensland, QLD 4069, Australia

The double-torsion test was employed to study the processes of crack propagation and to measure the fracture toughness of polycrystalline diamond. The value of fracture toughness of about 13 MPa $m^{1/2}$ is surprisingly high. Inhomogeneity in microstructure may cause discontinuous crack propagation which makes it difficult to study the subcritical crack growth behaviour of this polycrystalline material. Subcritical crack growth is shown to be negligible and crack deflection is shown to be an important toughening mechanism in polycrystalline diamond.

1. Introduction

Diamond is the hardest material known. The Knoop hardness of diamond ranges from about 55 to 113 GPa [1]. However, single-crystal diamond suffers from a susceptibility to easy fracture along the cleavage planes, especially the (1 1 1) plane. The solution to this problem is to sinter diamond powder into a large mass. The cleavage planes of the sintered diamond are randomly oriented, so massive fractures do not propagate easily through the material. This results in a significant increase in the fracture toughness of the sintered polycrystalline diamond compared with that of the single crystal.

Sintered diamond materials are widely used today as cutting elements in drilling bits, wire drawing dies, and other applications that need materials of supreme resistance to abrasive wear. Among these applications, polycrystalline diamond compacts (PDC) are used extensively as cutting elements on drag bits for drilling oil and gas wells. The PDC cutter was introduced by the General Electric Co. in 1972 [2]. The compact is a round disc comprising a thin layer of sintered polycrystalline diamond bonded to a cemented tungsten carbide substrate. Commercially available diamond compacts are usually made by sintering diamond powders in the temperature range 1500–2000 °C at pressures of 5–7 GPa using suitable metallic solvent/catalysts such as cobalt, iron, nickel and manganese [2, 3]. The catalyst metals play an important role in the sintering process. Direct bonding between diamond grains is very difficult to achieve when pure diamond powder is sintered without catalyst metals, even at a temperature as high as 2000 °C and a pressure of 7.7 GPa for 1 h [4].

Since diamond is much harder than tungsten carbide, PDC bits were introduced for drilling hard and abrasive formations which cemented carbide bits have difficulty in penetrating. In general, PDC bits have proved to be successful in drilling soft to medium hard formations such as shale, claystone, limestone, anhydrite, chalk and marl [5]. However, it turns out that PDC bits are susceptible to severe chipping and spalling when hard and abrasive formations are encountered [6]. In order to evaluate the resistance of PDC cutters to chipping failure, it would be useful to be able to measure the fracture toughness of the sintered diamond. The goals of this study were to develop a test procedure for measuring the fracture toughness of the polycrystalline diamond, and to study the fracture behaviour of this material.

2. The double-torsion test

Since large sintered diamond specimens are difficult to manufacture, conventional techniques cannot be employed to measure their fracture toughness. Two techniques are used commonly to determine the fracture toughness of diamond. One is to indent the surface of the samples by either Vickers indenter or blunt indenter [7, 8]. The other is a diametral compression test on a centre-notched disc [9–11]. Since the indenter is susceptible to damage in indenting the diamond surface (we did try and the Vickers diamond failed) and the stress state is somewhat complicated in a centre-notched disc, it was decided in this study to measure the fracture toughness of sintered diamond by using the double-torsion test. This specimen geometry is well suited to the planar form of the diamond layer in a PDC.

0022–2461

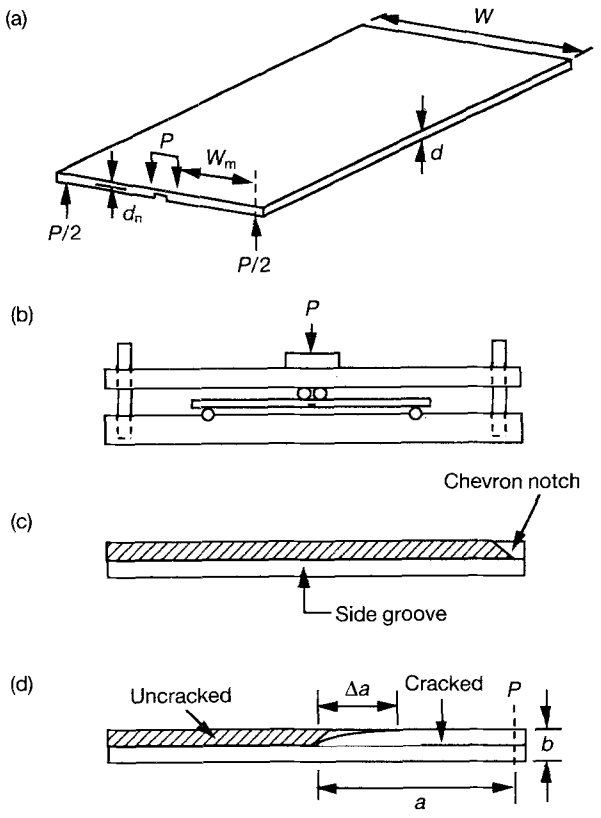

Figure 1 The double-torsion test. (a) Specimen configuration; (b) loading fixture; (c) side groove and chevron notch; (d) inclined crack front.

The double-torsion test was suggested by Outwater and developed by Kies and Clark [12]. One of the most comprehensive reviews of this technique was given by Tait *et al.* [13]. The typical specimen configuration and loading fixture are shown in Fig. 1. This technique has been extensively used to study the subcritical crack growth behaviour in such materials as glass, ceramics and cemented carbides, as well as minerals and rocks [12–19].

One of the most complete mathematical analyses of the technique was given by Williams and Evans [15]. The double-torsion specimen can be considered as two elastic torsion bars loaded with a load of $P/2$ (Fig. 1a). It has been shown that for small deflections, and for bars where the width is much greater than the specimen thickness, the stress intensity factor K_I is given by the following expression [15]:

$$K_I = PW_m\left(\frac{3}{Wd^3d_n(1-\nu)\varphi}\right)^{1/2} \quad (1)$$

for the plane strain condition, where P = total load applied to the specimen, W_m = moment arm, W = specimen width, d = specimen thickness, d_n = plate thickness in the plane of the crack (i.e. the web thickness) and ν = Poisson's ratio. φ is a correction factor for thick specimens obtained using elastic theory for thick plates, and is given by [20]

$$\varphi = 1 - 0.6302\frac{2d}{W} + 1.20\left(\frac{2d}{W}\right)e^{-\pi W/2d} \quad (2)$$

The stress intensity factor is thus a function of the applied load, specimen dimensions, and Poisson's ratio only. It is independent of the crack length*.

Using the relationship between the specimen compliance and the crack length, the rate of change of compliance can be related to the crack-growth rate. At constant displacement y in the load-relaxation technique (see next section), the crack-growth rate is related to the instantaneous load and the corresponding load-relaxation rate (i.e. dP/dt). It is given as [15]

$$\frac{da}{dt} = -\frac{Wd^3Gy}{3W_m^2P^2}\left(\frac{dP}{dt}\right) = -\frac{Wd^3E'y}{6W_m^2(1+\nu)P^2}\left(\frac{dP}{dt}\right) \quad (3)$$

where G and E' are the shear and Young's moduli of the material, respectively. Alternatively, the crack velocity can be obtained from the empirical relationship between the compliance of the double-torsion specimen and the crack length. It is given as [15]

$$\frac{da}{dt} = -\frac{P_i}{P^2}\left(a_i + \frac{D}{B}\right)\left(\frac{dP}{dt}\right) = -\frac{P_f}{P^2}\left(a_f + \frac{D}{B}\right)\left(\frac{dP}{dt}\right) \quad (4)$$

where B is the slope of the linear relation between the compliance and crack length and D is the intercept. The subscript i stands for the initial values of the load and crack length, and those with subscript f are the corresponding values at the completion of relaxation.

In general, except for very low modulus material, or for small crack lengths, $D/B \ll a_i$ so that

$$\frac{da}{dt} = -\frac{P_ia_i}{P^2}\left(\frac{dP}{dt}\right) = -\frac{P_fa_f}{P^2}\left(\frac{dP}{dt}\right) \quad (5)$$

Thus the crack velocity is obtained.

Since it is not necessary to measure the crack length of the specimen during the test, this experiment can be conducted conveniently on opaque materials such as sintered diamond, and in hostile environments, such as high temperature or corrosive media, where measurement of the crack length would be difficult.

3. Experimental procedure

An Instron testing machine model TM-M-L with a maximum load capacity of 980 N and a crosshead speed ranging from 0.05 to 100 mm min^{-1} was used to apply the compressive load to the specimens. The loading fixture was a four-point loading device, similar to that shown in Fig. 1b.

The specimens were obtained by grinding away the tungsten carbide backing from the PDC cutters, leaving circular plates of polycrystalline diamond approximately 0.7 mm thick and 25.4 mm (1 in.) to 50.8 mm (2 in.) in diameter. The plates were cut to a rectangular shape, and a central groove was spark-eroded along

* However, Trantina's [21] finite-element stress analysis showed that the independence of K_I values with respect to the crack length is valid only when $0.55W < a < L - 0.65W$. Shetty and Virkar [16] also obtained experimentally 3 cm $< a <$ 9 cm and 4 cm $< a <$ 7 cm for valid K_I values for specimens of dimensions 15.24 cm × 6.35 cm × 0.2 cm and 15.24 cm × 10.16 cm × 0.2 cm, respectively.

the length of the plates. A chevron-shaped starting notch then was spark-eroded through the plates (Fig. 1c).

Since the polycrystalline diamond discs are costly and difficult to produce, preliminary experiments were conducted on glass slides and alumina plates. This work was conducted to perfect the experimental technique and to validate the results by comparing them with those obtained using other techniques.

The glass specimens were microscope slides of dimensions 75 mm × 25 mm × 1 mm. No notch, but a slight scratch about 2 mm in length, was introduced at the end of the glass slides along the length direction. To introduce a sharp crack, the scratched glass slide was placed on the loading device and a compressive load was applied. When a crack was initiated it was allowed to propagate for a few millimetres, and then the load was released.

The alumina specimens, 99.5% polycrystalline alumina from Coors Ceramic Co., also had dimensions of 75 mm × 25 mm × 1 mm. A notch about 2 mm in length was cut by diamond saw at the end of the specimens along the length direction. The alumina specimens were also pre-cracked by loading them in the double-torsion loading fixture, and then unloading them as soon as a crack was initiated. This was determined when an abrupt drop in load occurred.

Typical load–displacement curves for tests on glass and alumina are shown schematically in Fig. 2. These curves are characterized by linear-elastic deformation to a peak load, at which point an atomically-sharp pre-crack is formed in the sample. Continued loading causes this crack to continue to propagate at a nearly constant load.

In order to obtain a diagram of crack velocity versus stress intensity factor, the load-relaxation technique at constant displacement was used. In the load-relaxation technique, a load P_i is applied to a precracked specimen at a high crosshead displacement rate. P_i is given a value of about 0.95 P_c, where P_c is the critical load which causes catastrophic failure of the specimen. The crosshead then is fixed and the load is allowed to relax. The crack velocity at each load can thus be obtained directly from the rate of load relaxation at the constant displacement and for given specimen dimensions or initial crack length via Equations 3 or 5. The corresponding values of stress intensity factor K_I then can be obtained from Equation 1. After the completion of load relaxation, the load is applied at a high crosshead displacement rate until catastrophic failure of the specimen to obtain P_c and thus K_{Ic}.

4. Experimental results

It has been well established that crack propagation in a corrosive environment can be described by a plot of crack velocity versus stress intensity factor (Fig. 3). In region I the crack propagation is controlled by the rate of the chemical reaction near the crack tip; in region II diffusion of the corrosive species to the crack tip is the rate-controlling factor; in region III the crack velocity is controlled by both the mechanical and chemical aspects [14].

Examples of the experimental results with glass and alumina are shown in Fig. 4. The results are reproducible and agree with results obtained by other workers [15]. The higher crack-growth rate for the double-torsion specimen is supposed by Evans [14]

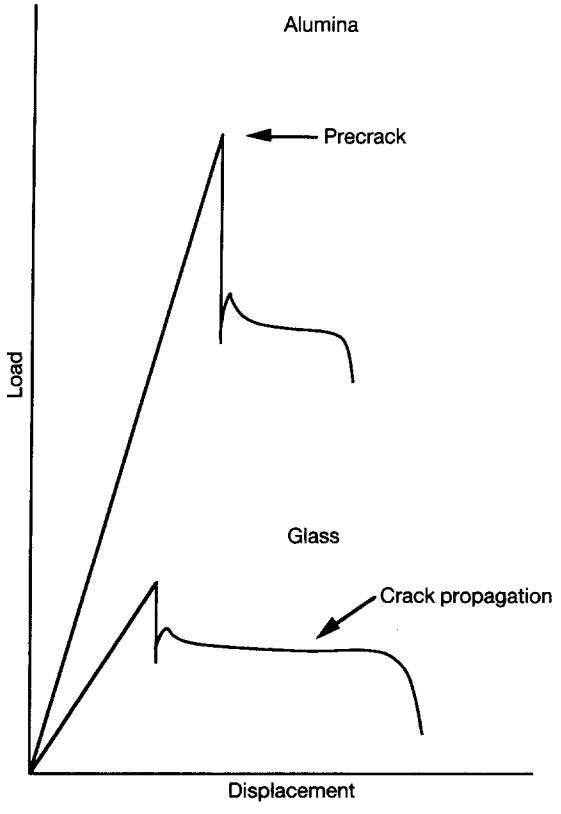

Figure 2 Schematic diagram showing typical load–displacement curves for double-torsion tests on (a) glass and (b) alumina.

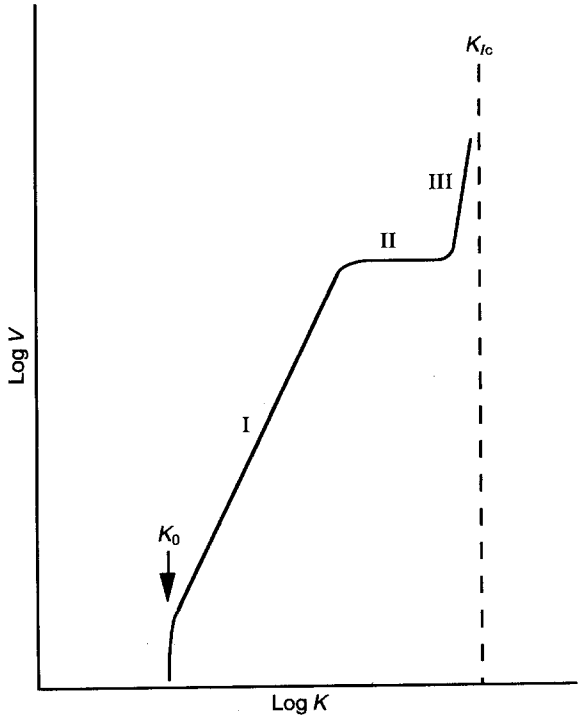

Figure 3 Crack velocity versus stress intensity factor.

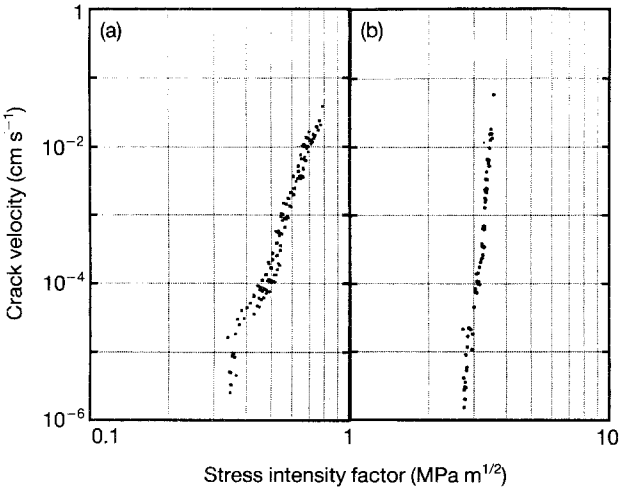

Figure 4 Subcritical crack propagation in glass and alumina in air.

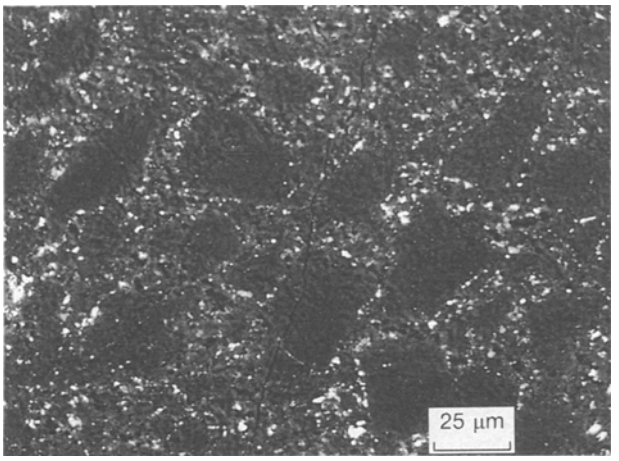

Figure 5 Backscattered electron image of sample No. 3.

and Williams and Evans [15] to arise because the crack-growth rate in Equation 3 (or 4) is overestimated due to the inclined crack front, and the crack-growth rate obtained should be reduced by a factor ϕ, where $\phi = b/(\Delta a^2 + b^2)^{1/2}$ (see Fig. 1d). After this correction, the data are in very good agreement. This gave us confidence to proceed with the experiments in the very expensive diamond samples.

Five diamond tables were tested and fracture toughness values were calculated. The loading rate for all of the samples was 0.05 mm min^{-1}. In sample No. 1, a pre-crack was developed when the load reached 123 N, at which point an abrupt drop in the applied load was observed and, when this occurred, the specimen was unloaded immediately. The sample then was reloaded and, on this second loading cycle, when the load reached 112 N again an abrupt drop in the applied load occurred and again the machine controls were adjusted to unload the specimen at this point. This process was repeated twice more before the specimen failed. The peak load values recorded during these cycles were 110 and 109 N. Using a Poisson's ratio value of 0.07 [11], the average value of fracture toughness was calculated as 14.28 MPa m$^{1/2}$.

Sample No. 2 was pre-cracked at a load of 125 N. The sample was unloaded following the formation of the pre-crack and then it was reloaded. In this case the sample behaved more like the alumina and glass samples. There was no abrupt drop in load observed in this sample and the crack propagated at a constant load of 101 N for about 1 s. At this point the sample again was unloaded. This procedure was repeated twice. The crack propagated when the loads reached the values of 100 and 93 N, respectively. The calculated stress intensity factor for this sample was 13.13 MPa m$^{1/2}$.

Sample No. 3 had dimensions of 29.50 mm × 14.58 mm × 0.69 mm. This sample showed coarse diamond grains (20–50 μm) embedded in a fine-grained diamond matrix (Fig. 5). It contained little cobalt. A pre-crack was developed when the load reached 89 N, at which point an abrupt drop in the applied load was observed and, when this occurred, the specimen was unloaded immediately and then was examined using a scanning electron microscope. The length of the crack on the tension side was around 0.7 mm while the crack opening displacement was less than 1 μm. This almost complete crack closure on removal of the load is evidence of very little plastic deformation of the polycrystalline diamond material. On the second loading cycle, when the load reached 84 N an abrupt drop in the applied load occurred and again the machine controls were adjusted to unload the specimen at this point. This process was repeated once more and the peak load recorded was 78 N. The average fracture toughness was calculated to be 13.43 MPa m$^{1/2}$.

Sample No. 4 had dimensions of 29.50 mm × 14.71 mm × 0.59 mm. It revealed a much more uniform microstructure than sample No. 3 (Fig. 6). The grain size of the diamond lay in the range of 5 to 15 μm. This sample contained a little more cobalt than sample No. 3. This sample was pre-cracked at a load of 70 N. The sample was unloaded following formation of the pre-crack and then was reloaded. There was no abrupt drop in load observed in this sample and the crack propagated at a constant load of 58 N for about 1.5 s before the specimen failed. The calculated fracture toughness for this sample was 13.03 MPa m$^{1/2}$.

Sample No. 5 had dimensions of 33.20 mm × 16.60 mm × 1.00 mm. This specimen contained diamond grains of 10–30 μm (Fig. 7). It seemed to have more cobalt than samples 3 and 4. This sample was pre-cracked at a load of 227 N. It was unloaded and then reloaded. The sample failed at a load of 176 N. The calculated stress intensity factor was 13.12 MPa m$^{1/2}$.

The results are summarized in Table I. It has to be mentioned that it was very difficult to control the direction of crack propagation so that it ran symmetrically down the mid-line of the sample. Great care was taken to manufacture the loading fixture and specimens very precisely, and to mount the latter as carefully as possible prior to the test. None the less all cracks, except in sample No. 1, deflected and went out of the guide groove during the pre-cracking proced-

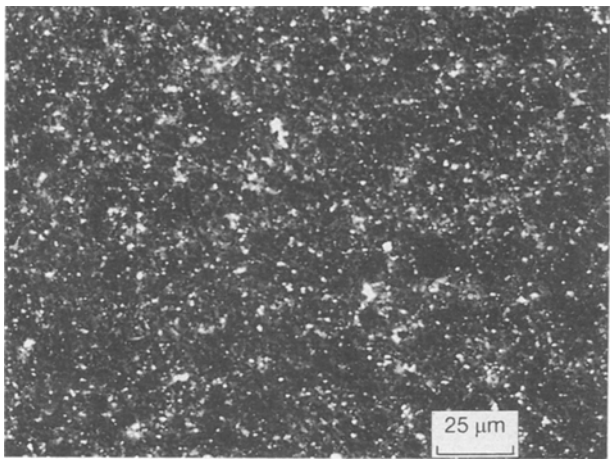

Figure 6 Backscattered electron image of sample No. 4.

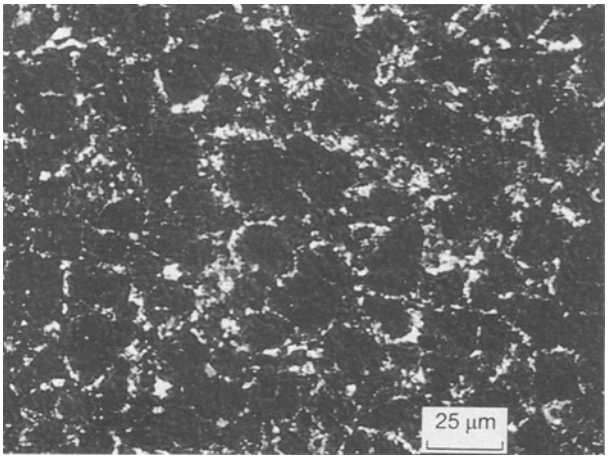

Figure 7 Backscattered electron image of sample No. 5.

TABLE I Results of double-torsion test on polycrystalline diamonds

Specimen No.	Number of tests	K_{Ic} (MPa $m^{1/2}$)	Standard deviation (MPa $m^{1/2}$)	Coefficient of variation (%)
1	3	14.28	0.20	1.4
2	3	13.13[a]	0.57	4.4
3	2	13.43	0.66	4.9
4	1	13.03[a]	–	–
5	1	13.12	–	–

[a] These two values were obtained from subcritical crack propagation. However, they should be very close to the critical stress intensity factor.

ure. Therefore total thickness, not web thickness, was used in the calculation of stress intensity factor for all specimens except sample No. 1.

5. Discussion

Although the diamond samples showed distinctive microstructures (Figs 5–7), the measured stress intensity values were very similar. Lammer [11] conducted Brazilian tests to measure the fracture toughness of cobalt-containing polycrystalline diamond. The specimens were 0.8 mm thick and 4 mm in diameter. A through-slot 2 mm long was cut at the centre of the discs. He reported fracture toughness values of 6.86–9.11 MPa $m^{1/2}$. In his tests, polycrystalline diamond with grain sizes in the range 10–40 μm seems to have a maximum fracture toughness. The values decrease with both decreasing and increasing nominal grain sizes of the diamond. These values are somewhat lower than, but of similar order of magnitude to, our results. The range of grain size distribution in the samples that were tested in this study was too small to show any variation of fracture toughness with the grain size distribution of the diamond.

Hibbs and Lee [22] investigated the wear scars of polycrystalline diamond compacts that were used to cut a cylindrical core of sandstone on a lathe. They found that some internal flaws such as poorly bonded grains or a defective crystal occasionally caused large fractures at the cutting edge during the cutting tests. Since, in sintered materials, larger grain-size specimens are more likely to have larger internal flaws, polycrystalline diamonds with smaller grain sizes are preferred. This hypothesis was confirmed by Lammer's [11] findings that the fracture toughness of polycrystalline diamond with larger nominal grain size (90–150 μm) is smaller than that with smaller grain size (10–40 μm).

In our SEM investigations of the cracked specimens, we found that the cracks usually deflect when a large diamond grain with no preferential cleavage is encountered (Fig. 8). Crack deflection is thus a significant toughening mechanism for sintered polycrystalline diamond. By contrast, cracks usually deflect locally along the cleavages of diamond crystals when the latter are favourably oriented (Fig. 9). No preferential crack path was found either along the diamond–diamond interfaces or in the cobalt phase.

It is interesting to note that the load–displacement curves for these diamond tables are quite different. Samples 1, 3 and 5 displayed a linear load–displacement relationship before an abrupt decrease in the applied load during crack propagation. The cracks did not propagate continuously but rather they

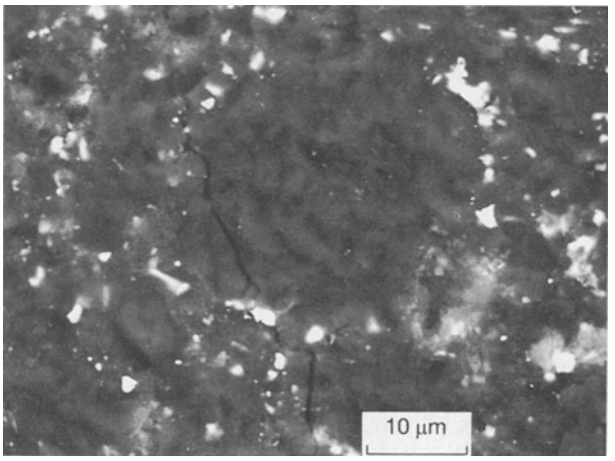

Figure 8 SEM micrograph showing crack deflection at a large diamond crystal (the general direction of the crack is from the bottom to the top).

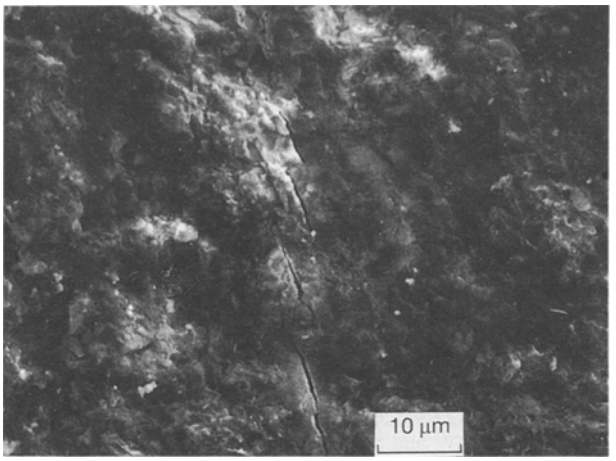

Figure 9 SEM micrograph showing a crack deflected locally along cleavages of a diamond crystal (the general direction of the crack is from the bottom to the top).

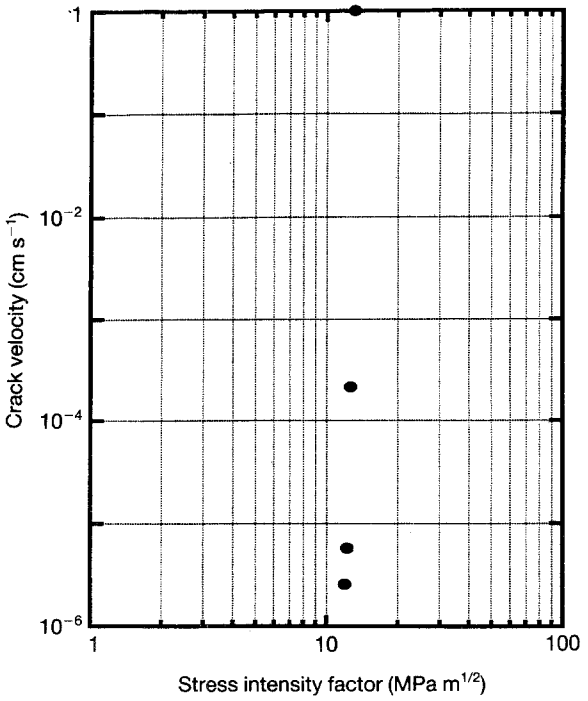

Figure 10 Subcritical crack propagation in sintered diamond in air.

proceeded in discrete jumps. Apparently, following each jump, the stress at the crack tip was relieved and additional load was needed to re-establish the critical stress intensity factor. This discontinuous crack propagation behaviour may be due either to the polycrystalline characteristic, i.e. inhomogeneity in the microstructure of the material, or to the presence of the cobalt phase. Hence it is very difficult to study the subcritical crack growth behaviour of the polycrystalline diamond.

On the other hand, sample No. 4 was much more homogeneous. The slope of the load–displacement curve began to decrease before the crack propagated at a constant stress intensity value of 13.03 MPa $m^{1/2}$. The decrease in the slope of the load–displacement curve was probably due to slow crack propagation. Therefore, though the fracture toughness values of the diamond samples tested are about the same, polycrystalline diamonds of poorly sorted grain size, i.e. samples 1, 3 and 5, may be preferable.

Slow crack-growth data are usually expressed as $V = AK_I^n$, where A and n are constants for a given material in a certain environment. A subcritical crack growth study of sintered polycrystalline diamond was conducted on sample No. 2 in air (Fig. 10). The slope of the curve in the V–K diagram is very steep. The value of the exponent n is around 90. This is to be expected since the sintered polycrystalline diamond is very brittle and corrosion-resistant. The range between the threshold and critical stress intensity values is very small, i.e. crack propagation occurs over a very narrow range of K_I values and subcritical crack growth in polycrystalline diamond is minimal.

6. Conclusions

Although a correction is needed for the crack velocity calculation based on the argument of the inclined crack front, and caution should be used regarding the length of the crack region from which the valid K_I values may be calculated, the double-torsion test is shown to be a simple and useful technique to measure the fracture toughness and study the slow crack-growth behaviour of materials in various environments. However, inhomogeneity in microstructure may cause discontinuous crack propagation which makes it difficult to study the subcritical crack growth behaviour of polycrystalline materials. In addition, in our experiments, most cracks in the test deflected and went out of the side groove during the pre-cracking procedure. High precision is needed in manufacturing the loading fixture, preparing the specimens, and aligning the specimens on the fixture.

Since cracks usually deflect when a large diamond grain with no preferential cleavage is encountered, crack deflection is a significant toughening mechanism in sintered polycrystalline diamond. It was found that diamond–diamond bonding is not less strong than the diamond crystal itself, particularly since the cleavage plane is the weak point in single-crystal diamonds and failure will occur on cleavage planes if they are favourably oriented. The exponent n in the V–K diagram for sintered polycrystalline diamond is very large. This implies that subcritical crack growth in this material is minimal, and that it is not susceptible to stress-corrosion effects in laboratory air.

Acknowledgements

We would like to thank the Hughes–Christensen company for providing a grant that supported this work. Messrs Redd H. Smith and Craig Cooley of the company are particularly appreciated for providing samples for the tests.

References

1. C. A. BROOKS, in "The Properties of Diamond", edited by J. E. Field (Academic, London, 1979) p. 383.
2. R. H. WENTORF, R. C. DEVRIES and F. P. BUNDY, *Science* **208** (1980) 873.

3. L. E. HIBBS Jr and R. H. WENTORF Jr, *High Temp.–High Press.* **6** (1974) 409.
4. M. AKAISHI, S. YAMAOKA, J. TANAKA, T. OHSAWA and O. FUKUNAGA, *J. Amer. Ceram. Soc.* **70** (1987) C237.
5. M. A. ARCENEAUX and J. L. FIELDER, in "Field Experience with PDC bits in North-East Texas", SPE paper 11390, presented at the SPE/IADC Annual Drilling Conference, New Orleans. Louisiana, USA, 20–23 Feb 1983 (SPE, Richardson) p. 273–8.
6. T. P. LIN, M. HOOD, G. A. COOPER and X. LI, *Wear* **156** (1992) 133.
7. B. LAWN and R. WILSHAW, *J. Mater. Sci.* **10** (1975) 1049.
8. T. NOMA and A. SAWOAKA, *J. Amer. Ceram. Soc.* **68** (1985) C271.
9. S. Ya. YAREMA, *Soviet Mater. Sci.* **12** (1976) 361.
10. L. N. DEVIN, A. L. MAISTRENKO, E. S. SIMKIN, S. I. SKLYAR and N. V. TSYPIN, *Soviet Powd. Metall. Metal Ceram.* **21** (1982) 419.
11. A. LAMMER, *Mater. Sci. Technol.* **4** (1988) 949.
12. J. A. KIES and A. B. J. CLARK, in Proceedings of 2nd International Conference on Fracture, Brighton, April 1969, edited by P. L. Pratt (Chapman & Hall, London, 1969) p. 483.
13. R. B. TAIT, P. R. FRY and G. G. GARRETT, *Exper. Mech.* **27** (1987) 14.
14. A. G. EVANS, *J. Mater. Sci.* **7** (1972) 1137.
15. D. P. WILLIAMS and A. G. EVANS, *J. Testg Eval.* **1** (1973) 264.
16. D. L. SHETTY and A. V. VIRKAR, *J. Amer. Ceram. Soc.* **61** (1978) 93.
17. B. J. PLETKA, E. R. FULLER Jr and B. G. KOEPKE, in "Fracture Mechanics Applied to Brittle Material", ASTM STP 678, edited by S. W. Freiman (American Society for Testing and Materials, Philadelphia, 1979) p. 19.
18. B. K. ATKINSON, *J. Geophys. Res.* **89** (B6) (1984) 4077.
19. K. J. CHEN and Y. C. KO, *Amer. Ceram. Soc. Bull.* **67** (1988) 1228.
20. E. R. FULLER Jr, in "Fracture Mechanics Applied to Brittle Materials", ASTM STP 678, edited by S. W. Freiman (American Society for Testing and Materials, Philadelphia, 1979) p. 3.
21. G. G. TRANTINA, *J. Amer. Ceram. Soc.* **60** (1977) 338.
22. L. E. HIBBS Jr and M. LEE, *Wear* **46** (1978) 141.

Received 26 May 1993
and accepted 21 March 1994